investigation in a crystalline basement terrain, southwestern Nigeria. *J. Environ. Earth Sci.*, 2010, **61**, 1481–1492.
6. Bentley, L. R. and Gharibi, M., Two- and three-dimensional electrical resistivity imaging at a heterogeneous site. *Geophysics*, 2004, **69**, 674–680.
7. Gharibi, M. and Bentley, L. R., Resolution of 3D electrical resistivity images from inversion of 2D orthogonal lines. *J. Environ. Eng. Geophys.*, 2005, **10**, 339–349.
8. Loke, M. H. and Barker, R. D., Rapid least-squares inversion of apparent resistivity pseudosections by a quasi-Newton method. *Geophys. Prospect*., 1996, **44**, 131–152.
9. Li, Y. and Oldenburg, D. W., Inversion of 3D DC resistivity data using an approximate inverse mapping. *Geophys. J. Int*., 1994, **116**, 527–537.
10. Park, S., Fluid migration in the vadose zone from 3D inversion of resistivity monitoring data. *Geophysics*, 1998, **63**, 41–51.
11. Chambers, J. E., Ogilvy, R. D., Meldrum, P. I. and Nissen, J., 3D electrical resistivity imaging of buried oil-tar contaminated waste deposits. *Eur. J. Environ. Eng. Geophys.*, 1999, **4**, 3–15.
12. Ogilvy, R., Meldrum, P. and Chambers, J., Imaging of industrial waste deposits and buried quarry geometry by 3D tomography. *Eur. J. Environ. Eng. Geophys.*, 1999, **3**, 103–113.
13. Aizebeokhai, A. P., Olayinka, A. I. and Singh, V. S., Numerical evaluation of 3D geoelectrical resistivity imaging for environmental and engineering investigations using orthogonal 2D profiles. *SEG Expanded Abstr.*, 2009, **28**, 1440–1444.
14. Aizebeokhai, A. P. and Olayinka, A. I., Anomaly effects of arrays for 3D geoelectrical resistivity imaging using orthogonal or parallel 2D profiles. *Afr. J. Environ. Sci. Technol.*, 2010, **4**, 446–454.
15. Aizebeokhai, A. P., Olayinka, A. I., Singh, V. S. and Uhuegbu, C. C., Effectiveness of 3D geoelectrical resistivity imaging using parallel 2D profiles. *Curr. Sci*., 2011, **101**, 1036–1052.
16. Nagaraja Rao, B. K., Rajurkar, S. T., Ramalingaswamy, G. and Ravindra Babu, B., Stratigraphy, structure and evolution of Cuddapah basin. *Geol. Soc. India Mem*., 1987, **6**, 33–86.
17. Jeyagopal, A. V., Raju, R. D., Maithani, P. B. and Chaki, A., Cyclic sedimentation and classification of the Papaghni Group of sediments, Cuddapah basin, Andhra Pradesh. *J. Geol. Soc. India*, 2008, **71**, 363–370.
18. Reddy, G. R. C., Ground water information Kadapa district, Andhra Pradesh, Southern Region, Central Groundwater Board, 2007, 1–47.
19. White, R. M. S., Collins, S., Denne, R., Hee, R. and Brown, P., A new survey design for 3D IP modelling at Copper hill. *Explor. Geophys.*, 2001, **32**, 152–155.
20. deGroot-Hedlin, C. and Constable, S. C., Occam's inversion to generate smooth two-dimensional models from magnetotelluric data. *Geophysics*, 1990, **55**, 1613–1624.
21. Sasaki, Y., Resolution of resistivity tomography inferred from numerical simulation. *Geophys. Prospect.*, 1992, **40**, 453–464.
22. Nagaraja Rao, B. K. and Ramalingaswamy, G., Some new thoughts on stratigraphy of Cuddapah Supergroup. *Seminar on Kaladgi-Badami, Bhima and Cuddapah Supergroup*, Mysore, India, 1976, pp. 17–20.

ACKNOWLEDGEMENTS. The Third World Academy of Science (TWAS), Italy in collaboration with the Council of Scientific and Industrial Research (CSIR), India acknowledged for providing Fellowship to first author for this study at the National Geophysical Research Institute (NGRI), Hyderabad, India. The second author thanks CSIR for Emeritus fellowship. Thanks are also due to Dr R. Rangarajan, Chief Scientist, NGRI and his colleagues for discussions and necessary help during field work.

Received 20 September 2012; revised accepted 13 June 2013

Quantification of gas hydrate and free gas in the Andaman offshore from downhole data

Maheswar Ojha* and Kalachand Sain

CSIR-National Geophysical Research Institute, Uppal Road, Hyderabad 500 007, India

Under Expedition-01 of Indian National Gas Hydrate Programme (NGHP Exp-01), drilling/coring was done in 2006 at one site in the Andaman Sea, where the base of gas hydrate stability, coinciding with the bottom simulating reflector (BSR) on seismic section, was observed at 610 m below sea floor (mbsf) with water depth of 1344 m. We estimate the saturation of gas hydrate and free gas by applying rock physics theories to downhole sonic velocity, and compare the results with the resistivity and chlorinity data. The result matches well with the pressure core data. Although the average saturation of gas hydrate is only 5% of pore volume (or 3% of sediment volume), the total amount of gas in the form of gas hydrate is about 1570.8 cubic metre within the sediментary column of 308 m above the BSR. The average concentration of free gas is estimated as ~1.4% of the pore volume within the sedimentary column of 80 m below the BSR.

Keywords: National Gas Hydrate Programme, quantification, rock physics.

ONE of the world's deepest and thickest gas hydrate-bearing zone was identified on the seismic data[1]. Drilling and coring were carried out at one site in the Andaman Sea during Expedition 01 of the Indian National Gas Hydrate Programme (NGHP Exp-01) for validating the ground truth of gas hydrate as inferred from seismic data (Figure 1). The Site NGHP-01-17 is located at 10°45.1912′N, 93°6.7365′E in the Andaman Sea, where coring along with wire line sonic, gamma ray, density and resistivity logging were carried out through sediments up to 691.6 m below the sea floor (mbsf) with water depth of ~1344 m (ref. 1). Very low geothermal gradient (19 ± 2°C per km) and high rate of sedimentation (~5.6 cm/kyr) led to thick gas hydrate zone in this area. The infrared (IR) thermal and porewater Cl^- anomalies at site 17 indicate gas hydrate within the ash-rich sediments between 250 to 608 mbsf where the bottom stimulating reflector (BSR), representing the base of gas hydrate stability field, has been observed on seismic section along a line passing through site 17 (ref. 1). Due to bad hole condition, good quality sonic velocity is available from ~300 mbsf, which has been used here to estimate the saturation of gas hydrate and free gas across the BSR. We

*For correspondence. (e-mail: maheswar_ojha@yahoo.com)

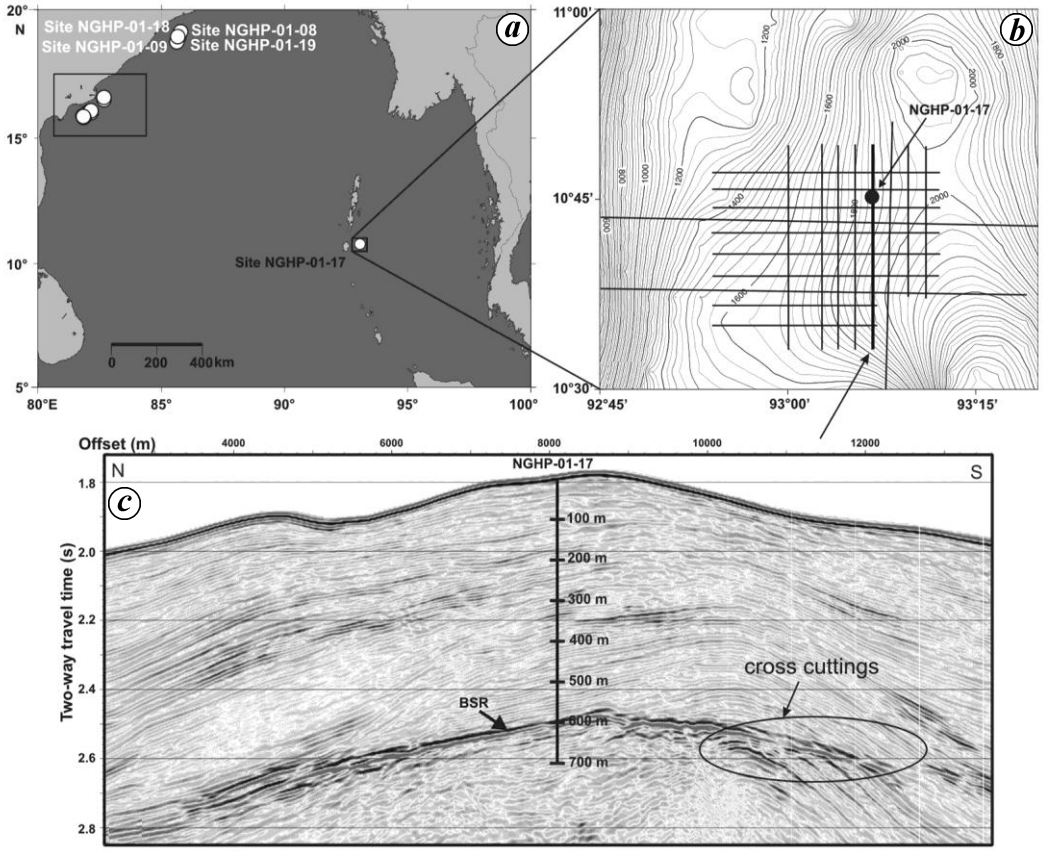

Figure 1. ***a***, Location of the Site NGHP-01-17 in the Andaman Sea. ***b***, Seismic profile is shown by the thick solid line crossing the site NGHP-01-17 (black dot); ***c***, Part of the seismic section showing the BSR at a depth of ~ 600 m below seafloor with opposite polarity with respect to the seafloor and cutting across the dipping strata (modified after Collett *et al.*[1]).

have also used the resistivity and chlorinity data for the quantification of gas hydrate, and compared the results with the pressure core measurements.

The Andaman Sea is an active backarc basin, located on the eastern edge of the Bay of Bengal (Figure 1 *a*). On the other hand, the Andaman Islands are volcanic island arc system located on the western edge of the Andaman Sea. The backarc system, comprising Indian, Burma and Sunda plate boundaries, were formed about 3 Ma ago[2], and the plates are being currently separated at a rate of 3.76 cm/year (ref. 3). The site NGHP-01-17 is situated between the Andaman Islands and the backarc spreading centre. Lithology of the Andaman Sea is dominated by terrigenous muddy clay (70–100%) from the Irrawaddy River, nannofossil carbonate ooze and minor amount of volcanic ashes, iron sulphide-rich zones and organic-rich intervals[4]. The 691.6 m sediment sequence of site 17 is predominated by nanno-fossil ooze with 382 m thin layers and patches of white, grey and black ash, white pumice fragments, and dispersed black ash and rare scoria of lapilli size[1]. The base of gas hydrate stability zone is predicted at 620 mbsf based on measured seafloor temperature of 5.6 ± 0.2°C and geothermal gradient of 19 ± 2°C per km assuming pure methane and pore water salinity of 35 ppt (refs 1 and 5).

Seismic velocity of pure solid gas hydrate is about 3.7 km/s, which is much higher than the background velocity (1.6–1.7 km/s) of shallow marine sediments. Therefore, presence of gas hydrate within the sediments increases seismic velocity. This increase in seismic velocity can be translated into the amount of gas hydrate using some rock physics modelling[6–16]. Here, we have used the three-phase Biot-type equation (TPBE)[17,18], which is very simple to apply and gives better results than other theories in the case of isotropic distribution of gas hydrate in marine sediments. The drilling, coring and wire line logging results show uniform sequence of 691.6 m thick sediment in which gas hydrate is distributed as pore fluid[1]. Therefore, assuming isotropic medium, the amount of gas hydrate can be estimated using the *P*-wave (V_P) and *S*-wave (V_S) velocities as

$$V_P = \sqrt{(K + 4\mu/3)/\rho_b} \text{ and } V_S = \sqrt{\mu/\rho_b},$$

where ρ_b is the bulk density of hydrate-bearing sediment.

The bulk (K) and shear (μ) moduli are determined as

$$K = K_m(1-\beta_1) + \beta_1^2 K_{av}$$

$$\mu = \mu_m(1-\beta_2)$$

$$\frac{1}{K_{av}} = \frac{\beta_1 - \phi}{K_m} + \frac{\phi_w}{K_w} + \frac{\phi_h}{K_h}$$

$$\beta_1 = \frac{\phi_a(1+\alpha)}{(1+\alpha\phi_a)},\ \beta_2 = \frac{\phi_a(1+\alpha\lambda)}{(1+\alpha\phi\gamma)},\ \gamma = \frac{(1+2\alpha)}{(1+\alpha)},$$

α is the consolidation parameter, *m*, *w* and *h* refer to sediment grain, water and hydrate respectively.

The apparent porosity, $\phi_a = \phi_w + \varepsilon\phi_h$; water-filled porosity, $\phi_w = (1 - S_h)\phi$; the hydrate-filled porosity, $\phi_h = S_h\phi$, where S_h is the hydrate saturation.

Here $\varepsilon = 0.12$, which accounts for the reduced impact of hydrate formation relative to compaction in terms of stiffening the host sediments' framework[18]. Here, $\alpha \approx 13.3(700/d)^{1/3}$, d is the depth below seafloor.

For comparison, we have estimated the saturation of gas hydrate using the Gassmann's formula[5], which is widely used for oil/hydrocarbon exploration. Gassmann's rock physics theory has been described in detail in previous works[19,20].

Here, we have used the porosity (ϕ, Figure 2 *a*) derived from downhole density (ρ_b) measurements using the standard density–porosity relation: $\phi = (\rho_g - \rho_b)/(\rho_g - \rho_w)$, where ρ_w (water density) and ρ_g (grain/matrix density) are taken as 1.03 and 2.66 g/cc respectively. The clay fraction (Figure 2 *b*) has been calculated from downhole gamma ray log by considering the minimum and maximum gamma ray values as 10 and 120 respectively. Figure 2 *c* and *d* display the resistivity and salinity variation as a function of depth. The *P*-wave velocity (Figure 2 *e*) used here is the wire line sonic. Several peaks observed in downhole data are due to very thin (less than 2 cm) consolidated carbonate ooze[1]. Other parameters used for the theoretical calculation are given in Table 1. Both the rock physics models have been calibrated with the velocity of water saturated sediment at a depth of 413.7 mbsf, where gas hydrates were not found in the pressure core. There are four pressure core measurements for gas hydrate and one for free gas. The pressure cores, collected *in situ* conditions followed by laboratory measurements, gives about 98% correct estimation.

Although Biot type and Gassmann's equation equally predict the velocity (Figure 2 *e*) of water-saturated sediment, the Gassmann's equation predicts higher hydrate saturation (Figure 2 *f*) than that of the Biot type theory[17,21]. This is probably because the Gassmann theory does not take into account stiffening of sediments due to presence of solid gas hydrate.

Pure gas hydrate is non-conductive and therefore increases the resistivity of sediments with increasing saturation of gas hydrate. The increase in resistivity against the background is converted into the amount of gas hydrate using the Archie's equation[22] as $S_h = (1 - S_w)$, where S_w is the water saturation in pore space and is expressed as $S_w = (R_0/R_t)^{1/n}$. $R_0 = aR_w/\phi^m$ is the resistivity of water saturated sediment, and R_w is the pore fluid resistivity as estimated from Fofonoff[23] by a linear fit to the *in situ* temperature profile using the measured seafloor temperature (5.5°C) and geothermal gradient of 20°C/km (ref. 1), and the water salinity, measured on interstitial water samples in this hole; ϕ is the sediment porosity, and R_t is the formation resistivity; $a = 2$, $m = 2.5$ and $n = 2$ (ref. 24) are called the Archie coefficient, cementation-exponent and saturation-exponent respectively. The saturation gas hydrate has been estimated using the spherically focused resistivity log (SFLU; Figure 2 *c*), which has the highest resolution but less depth of penetration. The saturation of gas hydrate with depth is shown by black solid line in Figure 2 *f*.

When sediment samples containing gas hydrate are brought to normal temperature and pressure conditions, gas hydrate dissociates and generates fresh water. Therefore, pore waters in the samples after dissociation of gas hydrate will be fresher than the *in situ* water[25] and the decrease in salinity can be used to quantify the amount of gas hydrate[26–28]. By assuming constant pore volume during the dissociation of gas hydrate, the saturation of gas hydrate, S_h can be measured from mass balance as[29,30]: $S_h = (C_{cb} - C_c)/C_{cb}$, where C_{cb} is the *in situ* 'baseline' pore water chlorinity and C_c is the chlorinity (salinity) measured (Figure 2 *d*) in the core sample after gas hydrate dissociation. Gas hydrate saturation estimated from chlorinity anomaly is shown by grey line in Figure 2 *f*.

From Figure 2 *f*, we conclude that the amount of gas hydrate estimated from the Biot-type equation best matches with the pressure core results (yellow dots) at this site NGHP-01-17. The average saturation of gas hydrate is estimated as 3% of sediment volume (5% of

Table 1. Various parameters used for theoretical calculation[14,32]

Parameters	Values with units
Bulk modulus of quartz	36 GPa
Shear modulus of quartz	45 GPa
Bulk modulus of clay	20.9 GPa
Shear modulus of clay	6.85 GPa
Bulk modulus of pure gas-hydrates	6.41 GPa
Shear modulus of pure gas-hydrates	2.54 GPa
Bulk modulus of water	2.25 GPa
Density of quartz	2.70 g/cc
Density of clay	2.60 g/cc
Density of pure gas-hydrates	0.92 g/cc
Density of seawater	1.03 g/cc
Critical porosity	0.62
Number of grain contacts	9

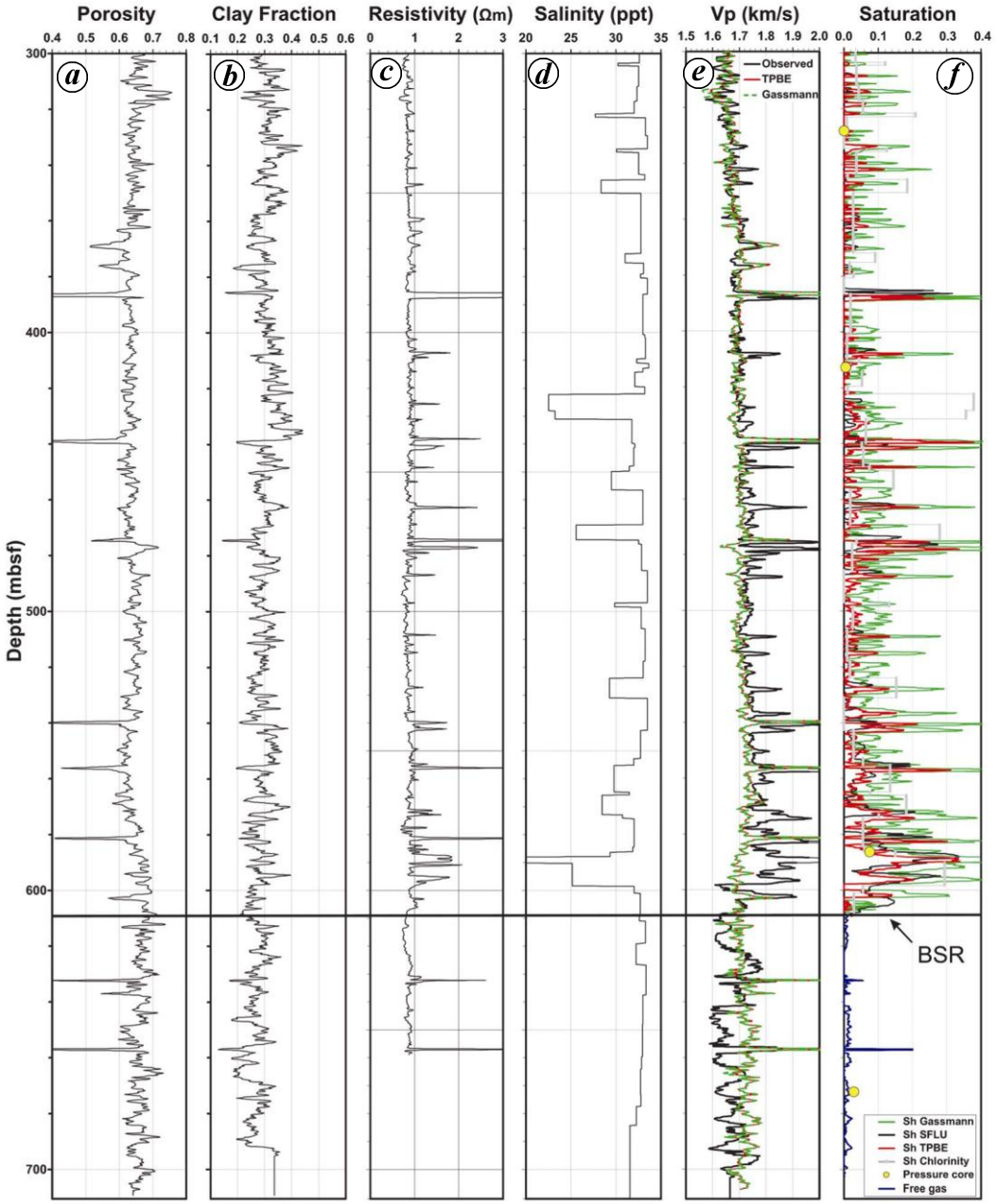

Figure 2. ***a***, Porosity calculated from wire line density; ***b***, Clay fraction using wire line gamma ray log; ***c***, SFLU resistivity; ***d***, Salinity of extracted water samples after dissociation of gas hydrate; ***e***, Observed wire line *P*-wave velocity (black line) along velocity of water saturated sediments (background velocity) using the TPBE (red line) and the Gassmann's (dotted green) equation; and ***f***, Hydrate saturation estimated using SFLU resistivity (black line), TPBE equation (red line), Gassmann's equation (green), pressure cores (yellow dots) and free gas saturation using Gassmann's equation (blue line).

pore volume) within 308 m sedimentary column, the total amount of gas below one unit surface area is estimated as 1570.8 cubic metre ($0.03 \times 308 \times 170$) by assuming 170 volume of gas dissociated from one volume of gas hydrate at normal pressure and temperature.

Presence of solid gas hydrate in pore spaces makes sediment impervious and acts as a trap for upcoming free gas. The seismic velocity of gas is very low and hence its presence decreases the *P*-wave velocity of the sediment drastically. We have estimated the saturation of free gas using the Gassmann's equation[5] by assuming uniform distribution of gas in the sediment pores. The theory has been described in detail in earlier studies[19,20]. As elastic properties of gas depend greatly on the pressure and temperature of the surrounding medium, we have corrected the density and bulk modulus of gas according to the rela-

tionship given by Batzle and Wang[31]. The density and bulk modulus of gas have been calculated as 0.262 g/cc and 0.114 GPa for pressure of 26.5 MPa and temperature of 20°C at BSR depth. The amount of free gas estimated here is shown by blue line in Figure 2 *f*.

We have incorporated the rock physics modelling to estimate the saturation of gas hydrate and free gas using the logging data in the Andaman Sea. The saturations estimated from various downhole logging and coring data demonstrate that the result based on rock physics modelling matches best with the pressure core measurements. Although the average saturation (5%) of gas hydrate is low, the total amount of gas as hydrate is very high due to large thickness (308 m) of hydrate-bearing sedimentary column.

1. Collett, T. *et al.* and the NGHP Expedition 01 Scientists, Indian National Gas Hydrate Program Expedition 01 Initial Reports. 2008, Directorate General of Hydrocarbons, Noida.
2. Curray, J. R., Possible greenschist metamorphism at the base of a 22-km sedimentary section, Bay of Bengal. *Geology*, 1991, **19**, 1097–1100.
3. Raju, K., Ramprasad, T., Rao, P. S., Rao, B. R. and Varghese, J., New insights into the tectonic evolution of the Andaman basin, northeast Indian Ocean. *Earth Planet. Sci. Lett.*, 2004, **221**, 145–162.
4. Colin, C., Kissel, C., Blamart, D. and Turpin, L., Magnetic properties of sediments in the Bay of Bengal and the Andaman Sea; impact of rapid North Atlantic Ocean climatic events on the strength of the Indian monsoon. *Earth Planet. Sci. Lett.*, 1988, **155**, 623–635.
5. Sloan, E. D., *Clathrate Hydrates of Natural Gases*, Marcel Dekker Inc., New York, 2nd edn, 1998, p. 628.
6. Gassmann, F., Elasticity of porous media: Über der Elastizität poröser Medien. *Vierteljahrsschrift der Naturforschenden Gesellschaft*, 1951, **96**, 1–23.
7. Lee, M. W., Hutchinson, D. R., Collett, T. S. and Dillon, W. P., Seismic velocities for hydrate-bearing sediments using weighted equation. *J. Geophys. Res.*, 1996, **101**, 20347–20358.
8. Lee, M. W. and Collett, T. S., Integrated analysis of well logs and seismic data to estimate gas-hydrate concentrations at Keathley Canyon, Gulf of Mexico. *Mar. Pet. Geol.*, 2008, **25**, 924–931.
9. Dai, J., Banik, N., Gillespie, D. and Dutta, N., Exploration for gas hydrates in the deepwater, northern Gulf of Mexico: Part II. Model validation by drilling. *Mar. Pet. Geol.*, 2008, **25**, 845–859.
10. Dvorkin, J., Prasad, M., Sakai, A. and Lavoie, D., Elasticity of marine sediments: rock physics modeling. *Geophys. Res. Lett.*, 1999, **26**, 1781–1784.
11. Dvorkin, J., Nur, A., Uden, R. and Taner, T., Rock physics of a gas hydrate reservoirs. *Leading Edge*, 2003, **22**, 842–846.
12. Ecker, C., Dvorkin, J. and Nur, A., Sediments with gas hydrate: internal structure from seismic AVO. *Geophysics*, 1998, **63**, 1659–1669.
13. Helgerud, M., Dvorkin, J., Nur, A., Sakai, A. and Collett, T., Elastic wave velocity in marine sediments with gas hydrates: effective medium modeling. *Geophys. Res. Lett.*, 1999, **26**, 2021–2024.
14. Jakobsen, M., Hudson, J. A., Minshull, T. A. and Singh, S. C., Elastic properties of hydrate-bearing sediments using effective medium theory. *J. Geophys. Res.*, 2000, **105**, 561–577.
15. Xu, H., Dai, J., Snyder, F. and Dutta, N., Seismic detection and quantification of gas hydrates using rock physics and inversion. In *Advances in Gas Hydrates Research* (eds Taylor, C. E. and Kwan, J. T.), Kluwer, New York, 2004, pp. 117–139.
16. Ghosh, R., Sain, K. and Ojha, M., Effective medium modeling of gas hydrate-filled fractures using sonic log in the Krishna–Godavari basin, offshore eastern India. *J. Geophys. Res.*, 2010, **115**, B06101.
17. Lee, M. W., Models for gas hydrate-bearing sediments inferred from hydraulic permeability and elastic velocities. *US Geol. Surv. Sci. Invest. Rep.*, 5219, 2008.
18. Lee, M. W. and Collett, T. S., Gas hydrate saturations estimated from fractured reservoir at Site NGHP-01-10, Krishna–Godavari Basin, India. *J. Geophys. Res.*, 2009, **114**, B07102.
19. Ojha, M. and Sain, K., Seismic velocities and quantification of gas-hydrates from AVA modeling in the western continental margin of India. *Mar. Geophys. Res.*, 2007, **28**, 101–107.
20. Ojha, M., *Quantitative Assessment of Gas Hydrate from Seismic Data*, Lambert Academic Publishing, Saarbrücken, Germany, 2012.
21. Ojha, M., Sain, K. and Minshull, T. A., Assessment of gas hydrate saturations in the Makran accretionary prism using the offset dependence of seismic amplitudes. *Geophysics*, 2010, **75**, C1–C6.
22. Archie, G. E., The electrical resistivity log as an aid in determining some reservoir characteristics. *Trans. Am. Inst. Min. Metall. Pet. Eng.*, 1942, **146**, 54–62.
23. Fofonoff, N. P., Physical properties of seawater: a new salinity scale and equation of state for seawater. *J. Geophys. Res.*, 1985, **90**, 3332–3342.
24. Pearson, C. F., Halleck, P. M., McGuire, P. L., Hermes, R. and Mathews, M., Natural gas hydrate deposits: a review of *in situ* properties. *J. Phys. Chem.*, 1983, **87**, 4180–4185.
25. Malinverno, A., Kastner, M., Torres, M. E. and Wortmann, U. G., Gas hydrate occurrence from pore water chlorinity and downhole logs in a transect across the northern Cascadia margin (Integrated Ocean Drilling Program Expedition 311). *Geophys. Res.*, 2008, **113**, B08103.
26. McDuff, R. E., Gieskes, J. M. and Lawrence, J. R., Interstitial water studies, Leg 42A, in Initial Rep. *Deep Sea Drill. Proj.*, 1978, **42**, 561–568.
27. Hesse, R. and Harrison, W., Gas hydrates (clathrates) causing porewater freshening and oxygen isotope fractionation in deep-water sedimentary sections of terrigenous continental margins. *Earth Planet. Sci. Lett.*, 1981, **55**, 453–462.
28. Kvenvolden, K. A. and Barnard, L. A., Gas hydrates of the Blake Outer Ridge, Site 533, Deep Sea Drilling Project Leg 76 in Initial Rep. *Deep Sea Drill. Proj.*, 1983, **76**, 353–365.
29. Ussler III, W. and Paull, C. K., Effects of ion exclusion and isotopic fractionation on pore water geochemistry during gas hydrate formation and decomposition. *Geol. Mar. Lett.*, 1995, **15**, 37–44.
30. Martens, C. S. and Berner, R. A., Methane production in the interstitial waters of sulfate-depleted marine sediments. *Science*, 1974, **185**, 1167–1169.
31. Batzle, W. and Wang, Z., Seismic properties of pore fluids. *Geophysics*, 1992, **57**, 1396–1408.
32. Lee, M. W. and Collett, T. S., Gas hydrate estimation error associated with uncertainties of measurement and parameters. *US Geol. Surv. Bull.*, 2182, 2001, Denver, Colorado.

ACKNOWLEDGEMENTS. We thank the Director, CSIR-NGRI for his permission to publish this work. The Directorate General Hydrocarbons and the Ministry of Earth Sciences are gratefully acknowledged for providing the data and financial support. We also thank the participants of the Indian NGHP Exp-01. This is a contribution to GENIAS Project of NGRI under the 12th Five Year Plan of CSIR.

Received 30 January 2013; revised accepted 10 June 2013